Geomechanics and Engineering, Vol. 2, No. 2 (2010) 141-156
DOI: http://dx.doi.org/10.12989/gae.2010.2.2.141

A radial point interpolation method for 1D contaminant transport modelling through landfill liners

*R. Praveen Kumar[1] and G.R. Dodagoudar[2]

[1]*Centre for Environmental Risk Assessment and Remediation, University of South Australia, Mawson Lakes, South Australia 5095, Australia*
[2]*Department of Civil Engineering, Indian Institute of Technology Madras, Chennai - 600 036, Tamil Nadu, India*

(Received August 31, 2009, Accepted June 16, 2010)

Abstract. In the framework of meshfree methods, a new methodology is developed based on radial point interpolation method (RPIM). This methodology is applied to a one-dimensional contaminant transport modelling in the saturated porous media. The one-dimensional form of advection-dispersion equation involving reactive contaminant is considered in the analysis. The Galerkin weak form of the governing equation is formulated using 1D meshfree shape functions constructed using thin plate spline radial basis functions. MATLAB code is developed to obtain the numerical solution. Numerical examples representing various phenomena, which occur during migration of contaminants, are presented to illustrate the applicability of the proposed method and the results are compared with those obtained from the analytical and finite element solutions. The proposed RPIM has generated results with no oscillations and they are insensitive to Peclet constraints. In order to test the practical applicability and performance of the RPIM, three case studies of contaminant transport through the landfill liners are presented. A good agreement is obtained between the results of the RPIM and the field investigation data.

Keywords: contaminant transport; meshfree method; radial point interpolation method; thin plate spline radial basis function; saturated porous media.

1. Introduction

A frequent use of land for the disposal of a wide variety of domestic and industrial wastes accentuates the importance of contaminant transport modelling in the porous media. Contaminants dispersed at the land surface migrate through the unsaturated and saturated porous media before reaching the groundwater. The rate at which the constituents of contaminants move through the porous media is determined by several transport mechanisms, including processes like advection, diffusion and dispersion, sorption and decay. Mass conservation statements of these processes lead to the governing equation of contaminant transport. Generally, contaminant movement in the porous media is predicted using analytical, physical, field and numerical models. For solving transport problems having simplified boundary conditions and geometries, exact analytical solutions are available in the literature (van Genuchten 1981, Rowe and Booker 1985). Physical and field models

*Corresponding author, Research Associate, E-mail: praveen.rachakonda@unisa.edu.au

are generally cumbersome and difficult to use in practice.

The use of robust numerical models in analyzing the problems of contaminant transport has been increased continuously, as they are able to accommodate the complexity of the domain and various types of boundary conditions. Many researchers have proposed various numerical models for solving the governing equation of contaminant transport (Pinder and Gray 1977, Frind 1988, Zheng and Bennet 1995, Eldho and Rao 1997, Craig and Raideau 2006). It should be noted that for high values of Peclet number, numerical oscillations will arise and special techniques such as artificial viscosity, upwinding, etc. must be developed to obtain accurate solution of the advection-diffusion equation in the case of conventional finite element analyses (Donea and Huerta 2003). In the finite element method, oscillations can be removed by mesh and time step refinement which clearly undermine the practical utility of the method. However, the stabilizing schemes such as characteristic based split (CBS) algorithm and time stepping schemes such as Discontinuous Galerkin can be used to overcome numerical oscillations. This has motivated the development of alternative numerical methods, which preclude oscillations without requiring mesh or time step refinement.

In recent years, a group of new methods called meshfree methods, such as the element free Galerkin method (Belytschko *et al*. 1994), the smooth particle hydrodynamics (Monaghan 1998), the reproducing kernel particle method (Liu *et al.* 1995), the radial point interpolation method (Wang and Liu 2002) and others, have been developed; whose main aim is to eliminate the structure of the mesh and construct the approximate solutions for the discrete equation entirely in terms of a set of nodes. Among all the meshfree methods, the radial point interpolation method (RPIM) has been successfully used for solving numerous boundary-value problems related to various fields of study (Wang *et al.* 2002, Li *et al.* 2003, Dai *et al.* 2004, Liu *et al.* 2005, Praveen Kumar 2008, Praveen Kumar and Dodagoudar 2008).

Boztosun and Charafi (2002) presented a meshfree method for solving the advection-diffusion equation using collocation method with thin plate radial basis functions. Li *et al.* (2003) developed an algorithm based on meshfree method for modelling the groundwater contaminant transport using collocation method with radial basis functions. Praveen Kumar *et al.* (2007) and Praveen Kumar and Dodagoudar (2008) developed a methodology based on RPIM to model contaminant transport through the saturated and unsaturated porous media. It is seen that a limited amount of research is undertaken regarding the potential usage of the meshfree methods for modelling contaminant transport processes in the saturated porous media. Hence, there is a need to understand the meshfree methods and to formulate a numerical model properly for analyzing the migration of contaminants through the porous media and landfill liners.

In the present study, a methodology is developed for modelling one-dimensional advection-dispersion equation involving first-order degradation through the saturated porous media using the RPIM. In this paper, thin plate spline radial basis functions (TPS-RBFs) proposed by Liu *et al.* (2005), for solving solid mechanics problems, are made use of in the analysis. MATLAB code is developed for modelling the contaminant migration using the RPIM. Results of the RPIM analysis are compared with analytical solutions, finite element results and field investigation data and found to be satisfactory.

2. Radial point interpolation method

The Radial Point Interpolation Method (RPIM) (Wang and Liu 2002) is a meshfree method

developed using the Galerkin weak form and the radial basis shape functions that are constructed based only on a group of nodes arbitrarily distributed in a local support domain by means of interpolation (Liu *et al.* 2005). For solving integrals in the weak form formed due to the Galerkin approximation procedure, a background mesh is used. Since the RPIM shape functions satisfy the Kronecker delta function property, the enforcement of essential boundary conditions is simple in the RPIM as in the case of finite element method.

2.1 Formulation using radial polynomial basis

Consider a continuous function $C(x)$ defined on a domain $\Omega \subseteq \Re^K$, where $K = 1$. Let $\Omega_x \subseteq \Omega$ denote a sub-domain describing the neighbourhood of a point, $x \in \Re^K$ located in Ω. According to the RPIM with polynomial reproduction, the approximation, $C^h(x)$ of $C(x)$ is (Wang and Liu 2002)

$$C^h(x) = \sum_{i=1}^{N} R_i(x)a_i + \sum_{j=1}^{m} p_j(x)b_j = \boldsymbol{R}^T(x)\boldsymbol{a} + \boldsymbol{p}^T(x)\boldsymbol{b} \tag{1}$$

where a_i is the coefficient for the radial basis $R_i(x)$ and b_j is the coefficient for the polynomial basis $p_j(x)$, N is the number of nodes in an influence domain of x, and m is the polynomial term which is usually $m < N$. Addition of the polynomial term improves the accuracy of the interpolation. The vectors are defined as

$$\begin{aligned} \boldsymbol{p}^T(x) &= [p_1(x), p_2(x), \ldots, p_m(x)] \\ \boldsymbol{R}^T(x) &= [R_1(x), R_2(x), \ldots, R_N(x)] \end{aligned} \tag{2}$$

Thin plate spline radial basis is a function of distance r_i and is defined as follows

$$\begin{aligned} \boldsymbol{R}_i(x) &= \boldsymbol{R}_i(r_i) = [(x - x_i)^2]^q \\ r_i &= \sqrt{(x - x_i)^2} \end{aligned} \tag{3}$$

where q is the shape parameter of the thin plate spline radial basis function.

Polynomial basis has the following monomial terms

$$\boldsymbol{p}^T(x) = [1, x] \tag{4}$$

The coefficients a_i and b_j are determined by enforcing the interpolation function pass through all N scattered points within the influence domain (Fig. 1). The matrix form of Eq. (1) is expressed as

$$\boldsymbol{C}^e = \boldsymbol{R}_Q\boldsymbol{a} + \boldsymbol{P}_m\boldsymbol{b} \tag{5}$$

where $\boldsymbol{C}^e = [C_1, C_2, C_3, \ldots, C_N]^T$

The moment matrices corresponding to the radial basis function $\boldsymbol{R}_Q$ and the polynomial basis function $\boldsymbol{P}_m$ are given by

$$\boldsymbol{R}_Q = \begin{bmatrix} R_1(r_1) & R_2(r_1) & \cdots & R_N(r_1) \\ R_1(r_2) & R_2(r_2) & \cdots & R_N(r_2) \\ \vdots & \vdots & \vdots & \vdots \\ R_1(r_N) & R_2(r_N) & \cdots & R_N(r_N) \end{bmatrix}_{N \times N} ; \quad \boldsymbol{P}_m = \begin{bmatrix} p_1(x_1) & p_2(x_1) & \cdots & p_m(x_1) \\ p_1(x_2) & p_2(x_2) & \cdots & p_m(x_2) \\ \vdots & \vdots & \vdots & \vdots \\ p_1(x_N) & p_2(x_N) & \cdots & p_m(x_N) \end{bmatrix}_{N \times m} \tag{6}$$

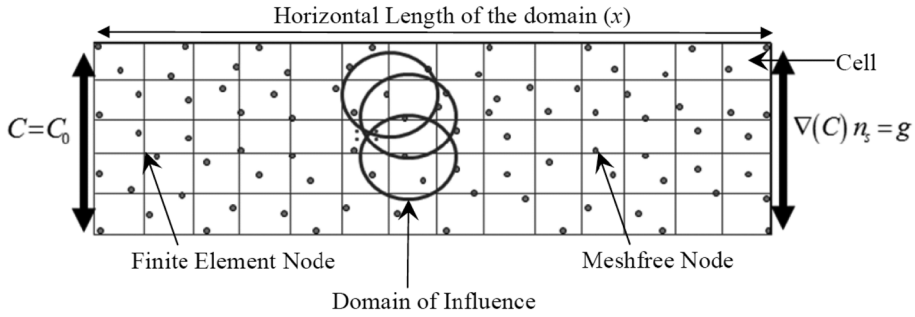

Fig. 1 Schematic of the problem domain

There are altogether ($N + m$) coefficients to be determined whereas only N equations are available above. To guarantee the unique solution, the following constraints are imposed

$$\sum_{i=1}^{N} p_j(x_i)a_i = \boldsymbol{P}_m^T\boldsymbol{a} = 0,\ j = 1, 2, \ldots, m \tag{7}$$

Combining Eqs. (5) and (7)

$$\begin{bmatrix} \boldsymbol{R}_Q & \boldsymbol{P}_m \\ \boldsymbol{P}_m^T & \boldsymbol{0} \end{bmatrix} \begin{Bmatrix} \boldsymbol{a} \\ \boldsymbol{b} \end{Bmatrix} = \begin{Bmatrix} \boldsymbol{C}^e \\ 0 \end{Bmatrix} \tag{8}$$

The unique solution for vectors of coefficients $\boldsymbol{a}$ and $\boldsymbol{b}$ is obtained by solving Eq. (8) and they are expressed as

$$\begin{aligned} \boldsymbol{b} &= \boldsymbol{S}_b\boldsymbol{C}^e \\ \boldsymbol{a} &= \boldsymbol{S}_a\boldsymbol{C}^e \end{aligned} \tag{9}$$

where

$$\begin{aligned} \boldsymbol{S}_b &= [\boldsymbol{P}_m^T\boldsymbol{R}_Q^{-1}\boldsymbol{P}_m]^{-1}\boldsymbol{P}_m^T\boldsymbol{R}_Q^{-1} \\ \boldsymbol{S}_a &= \boldsymbol{R}_Q^{-1}[\boldsymbol{1} - \boldsymbol{P}_m\boldsymbol{S}_b] \end{aligned} \tag{10}$$

The interpolation for $C(x)$ is expressed as

$$C(x) = [\boldsymbol{R}^T\boldsymbol{S}_a + \boldsymbol{P}^T\boldsymbol{S}_b]\boldsymbol{C}^e = \boldsymbol{\Phi}(x)\boldsymbol{C}^e \tag{11}$$

where the matrix of shape functions is defined as

$$\boldsymbol{\Phi}(x) = [\phi_1(x), \phi_2(x), \ldots, \phi_N(x)] \tag{12}$$

The derivatives of shape function are

$$\frac{\partial \phi_k}{\partial x} = \sum_{i=1}^{N} \frac{\partial R_i}{\partial x}\boldsymbol{S}_a + \sum_{j=1}^{m} \frac{\partial p_j}{\partial x}\boldsymbol{S}_b \tag{13}$$

where $\dfrac{\partial R_i}{\partial x} = 2q(r_i^2)^{q-1}(x - x_i)$

3. Discretisation of governing equation

The one-dimensional form of the governing equation for contaminant migration through the saturated porous media is expressed as

$$\left(1+\frac{\rho_d}{n}K_d\right)\frac{\partial C}{\partial t} = D\frac{\partial^2 C}{\partial x^2} - \left(\frac{u}{n}\right)\frac{\partial C}{\partial x} - \alpha C \tag{14}$$

The governing Eq. (14) must be complemented with initial and boundary conditions. They are

$$C(x, 0) = C_i \quad \forall x \in \Omega \tag{15a}$$

$$C(0, t) = C_0 \text{ on } \Gamma_S \text{ (Dirichlet boundary conditions)} \tag{15b}$$

$$\frac{\partial C}{\partial x} n_S = g \text{ on } \Gamma_E \text{ (Neumann boundary conditions)} \tag{15c}$$

where n is the porosity of the soil, ρ_d is the bulk density of the soil [ML^{-3}], C is the concentration of contaminant [ML^{-3}], D is the hydrodynamic dispersion coefficient [L^2T^{-1}], u is the discharge velocity [LT^{-1}], K_d is the distribution coefficient [L^3M^{-1}], α is the decay coefficient [T^{-1}], C_0 and g are the concentration of contaminant at the source [ML^{-3}] and the concentration gradient at the exit boundary respectively, n_S is the unit normal to domain Ω and, Γ_S and Γ_E are the portions of boundary Γ where the source concentration and the concentration gradient are prescribed.

The weak form of Eq. (14) is expressed as

$$\int_0^L \delta C^T D\frac{\partial^2 C}{\partial x^2}dx - \int_0^L \delta C^T\left(\frac{u}{n}\right)\frac{\partial C}{\partial x}dx - \int_0^L \delta C^T\left(1+\frac{\rho_d}{n}K_d\right)\frac{\partial C}{\partial t}dx - \int_0^L \delta C^T\ \alpha\ C\ dx = 0 \tag{16}$$

where L is the length of the domain.

By using divergence theorem, Eq. (16) can be written as

$$\begin{aligned}&\int_0^L \delta\left(\frac{\partial C^T}{\partial x}\right)D\frac{\partial C}{\partial x}dx + \int_0^L \delta C^T\left(\frac{u}{n}\right)\frac{\partial C}{\partial x}dx \\ &\quad + \int_0^L \delta C^T\left(1+\frac{\rho_d}{n}K_d\right)\frac{\partial C}{\partial t}dx + \int_0^L \delta C^T\alpha\ C\ dx = \delta C^T\ D\frac{\partial C}{\partial x}n_S\Big|_{\Gamma_E}\end{aligned} \tag{17}$$

By using Eqs. (11) and (12) in the discretisation of Eq. (17), the following relationship is obtained

$$[\boldsymbol{K}^{(1)}]\{\boldsymbol{C}\} + [\boldsymbol{K}^{(2)}]\{\boldsymbol{C}\}_{,t} = \{\boldsymbol{Q}\} \tag{18}$$

where

$$\begin{aligned}\boldsymbol{K}_{IJ}^{(1)} &= \int_0^L \left[\Phi_{I,x}^T D\Phi_{J,x} + \Phi_I^T\left(\frac{u}{n}\right)\Phi_{J,x}^T + \Phi_I^T\alpha\Phi_J\right]dx \\ \boldsymbol{K}_{IJ}^{(2)} &= \int_0^L \left[\Phi_I^T\left(1+\frac{\rho_d}{n}K_d\right)\Phi_J\right]dx \\ \boldsymbol{Q}_I &= \Phi_I^T\ D\ g|_{\Gamma_E}\end{aligned} \tag{19}$$

where Φ is the shape function.

Using Crank-Nicolson method for time approximation, Eq. (18) reduces to

$$\boldsymbol{K}_{new}\boldsymbol{C}_n = \boldsymbol{R}_n \tag{20}$$

where

$$\begin{aligned}
\boldsymbol{K}_{new} &= \boldsymbol{K}^{(1)^*} + \boldsymbol{K}^{(2)} \\
\boldsymbol{R}_n &= \left([\boldsymbol{K}^{(2)}] - \frac{\Delta t}{2}[\boldsymbol{K}^{(1)}]\right)\{\boldsymbol{C}\}_{n-1} + \frac{\Delta t}{2}(\{\boldsymbol{Q}\}_n + \{\boldsymbol{Q}\}_{n-1}) \\
\boldsymbol{K}^{(1)^*} &= \frac{\Delta t}{2}[\boldsymbol{K}^{(1)}]
\end{aligned} \tag{21}$$

where C_n and C_{n-1} are the nodal concentrations and $\boldsymbol{Q}_n$ and $\boldsymbol{Q}_{n-1}$ are the nodal mass fluxes at start and end of the time increment respectively.

4. Numerical examples: results

For all the numerical examples, it is assumed that the porous medium in which the contaminants move is homogenous and the source of contaminant is continuous. To illustrate the applicability of the RPIM, two validation examples and one numerical example dealing with the processes occurring in the porous media during the transport are considered and the findings are compared with the analytical solutions and finite element results. Based on the parametric study conducted by the authors, for modelling contaminant transport through the saturated and unsaturated porous media using RPIM, it can be stated that the shape parameter "q" is problem dependent. In the RPIM, a linear basis function is used for constructing the shape functions and the TPS-RBFs. Based on the results of the parametric study conducted for the example problems as well as for the case studies presented in the article, it is found that $q \approx 1.25$ (range 1.0-3.5; Wang and Liu 2002) has produced acceptable results.

In the first validation example, the results obtained from the present method are compared with the findings of Li *et al.* (2003). In second validation example, the results obtained from the RPIM are compared with those of Boztosun and Charafi (2002). In numerical example 1, the results obtained from the RPIM and finite element method (FEM) are compared with the analytical solution for an advection dominant problem. In all the above example problems, nodes of the background mesh are chosen to be coincident with the meshfree nodes.

4.1 Validation with published data: pure diffusion

When the seepage velocity (v) is low (*e.g.*, contaminant transport through the geosynthetic clay liner in landfill), diffusion tends to dominant advection and hence the advective transport can be ignored (Rowe and Booker 1985). This example deals with the transport of contaminant by pure diffusion only.

The RPIM is applied to the problem considered by Li *et al.* (2003). The model is applied to a soil column of horizontal length of 100 units with the initial condition $C\ (x,\ 0) = 0$ and the boundary conditions $C\ (x,\ t) = 1.0$ units at $x = 0$ and $\partial C(x, t)/\partial x = 0$ at $x = 100$ units. The coefficient of

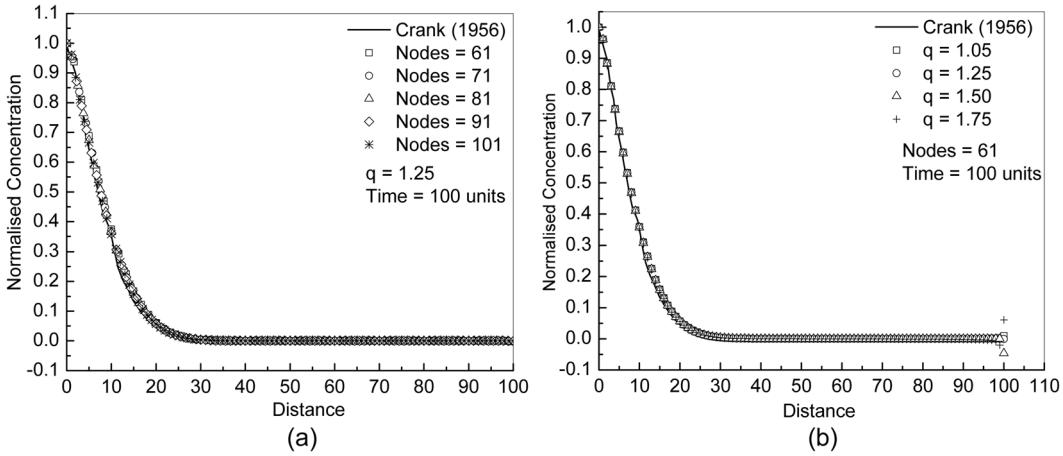

Fig. 2 Concentration profiles for different (a) meshfree nodes (b) q values (Pure Diffusion)

hydrodynamic diffusion (D) is taken as 0.5 units. The simulation has been carried out for 100 units with a time step of 0.1 units. The analytical solution for this case was given by Crank (1956) as

$$C = C_0 erfc\left(\frac{x}{\sqrt{4Dt}}\right) \tag{22}$$

In order to study the influence of number of meshfree nodes on the predicted results, a parametric study is conducted with nodes varying from 61 to 101 with an increment of 10. From the results (Fig. 2(a)), it is noted that convergent results are obtained using 61 meshfree nodes. Though more convergent results are being obtained with more meshfree nodes, the results with 61 nodes are practically acceptable. Fig. 2(b) depicts the concentration profiles with distance for various values of shape parameter (q). It is seen from the figure that the results are almost invariant in the initial reach but at the far reach region, there is a variation in the values of concentrations. For further analysis, the shape parameter q is taken as 1.25, which is evident from the figure. From Fig. 3, it is

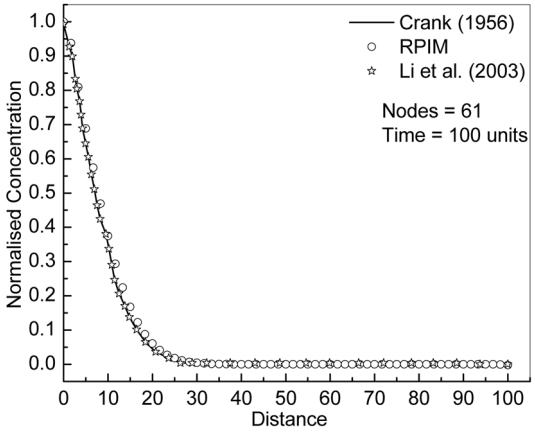

Fig. 3 Comparison of RPIM and Li *et al.* model results with analytical solution (Pure Diffusion)

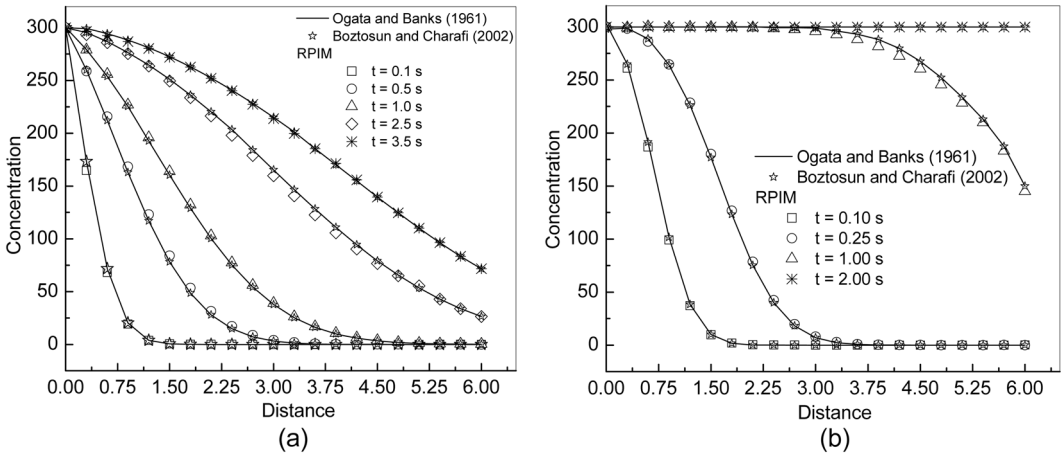

Fig. 4 Comparison of RPIM and Boztosun and Charafi model results with analytical solution for (a) D = 1 unit and v = 1 unit (b) D = 1unit and v = 6 units (Advection-Dispersion)

observed that both the RPIM and analytical results, as well results from Li *et al.* (2003) are in agreement with one another.

4.2 Validation with published data: advection-dispersion

This example deals with the modelling of plume developed due to advection-dispersion process. Boztosun and Charafi (2002) considered a one-dimensional advection-diffusion problem with initial condition C (x, 0) = 0 and boundary conditions C (x, t) = 300 units at x = 0 and $\partial C(x, t)/\partial x = 0$ at x = 6 units. The proposed RPIM is applied to this problem. The parameters considered in the analysis are: seepage velocity (v) = 1 unit and 6 units, coefficient of hydrodynamic diffusion (D) = 1. The analytical solution given by Ogata and Banks (1961) is

$$C = \frac{C_0}{2}\left[erfc\left(\frac{x - vt}{2\sqrt{Dt}}\right) + \exp\left(\frac{v\,x}{D}\right) erfc\left(\frac{x + vt}{2\sqrt{Dt}}\right)\right] \tag{23}$$

The problem domain [0, 6] is discritised into 21 cells and the shape parameter q is taken as 1.25. A comparison between the results obtained from the RPIM and Boztosun and Charafi (2002) with that of analytical solution at different time steps is shown in Fig. 4. From figure, it is noted that both the RPIM and analytical results, as well results from Boztosun and Charafi model are in good agreement.

4.3 Example 1: advection-dispersion (advection dominant case)

This example presents the case of a contaminant transport for which advection is highly dominant [Peclet number (P_e) = 20 and 200]. The RPIM is applied for a column of horizontal length of 50 cm with initial condition C (x, 0) = 0 and boundary conditions C (x, t) = 1 mg/L at x = 0 cm and $\partial C(x, t)/\partial x = 0$ at x = 50 cm. The parameters considered in the analysis are: $u = 1.0 \times 10^{-2}$ cm/s; n = 0.368 and dispersivity of soil (α) = 0.1 cm and 0.01cm for the two Peclet numbers, respectively.

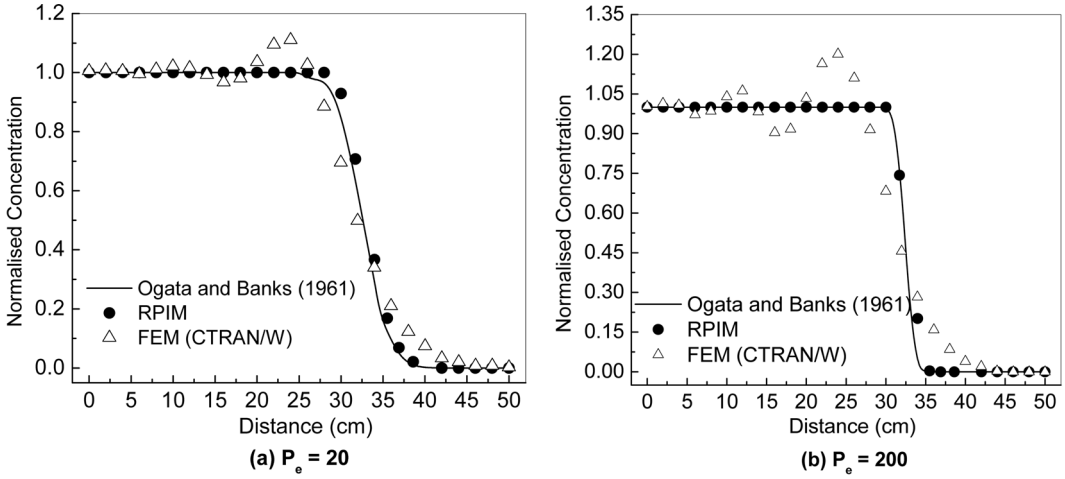

Fig. 5 Comparison of results of FEM and RPIM with analytical solution for (a) P_e = 20 and (b) P_e = 200 (Example 1: Advection-Dispersion)

The problem domain [0-50 cm] is divided into 26 uniformly spaced meshfree nodes with 25 cells. The simulation has been carried out for 20 minutes with a time step of 1 minute. Peclet number can be defined as the ratio between advective flow and flow due to dispersion. It is represented as

$$P_e = \frac{v\Delta x}{D} \tag{24}$$

where v = seepage velocity = u/n, Δx = grid length, D = hydrodynamic dispersion coefficient = αv.

A finite element package, CTRAN/W (2007) is also used for solving this example problem and the results are compared with that of the RPIM. In the finite element analysis, domain is discritised into 25 elements with 26 nodes. A comparison between the results obtained from the RPIM and FEM with that of the analytical solution at different P_e is shown in Fig. 5. The results obtained from the proposed RPIM model for advection dominated problem are in good agreement with the analytical solution. Thus, it ensures that the present model is free from numerical oscillations and insensitive to Peclet constraints.

The sharpness of the concentration front, or the degree to which the transport problem is dominated by advection, can be measured by the grid Peclet number. Conventional numerical methods require the smaller grid size in order to avoid the artificial oscillations arising out of overshoot or undershoot in the case of advection-dominated problems. Use of smaller grid spacing may be impractical for a large problem in terms of computer memory and execution. The Peclet number is dependent on mesh/grid size. The problem of artificial oscillations can be overcome through the use of meshfree methods. The meshfree methods do not involve mesh, so the methods are insensitive to Peclet constraints. It is seen from the present example that the results obtained from the RPIM are free from numerical oscillations for advection-dominated problems and thus insensitive to Peclet constrains. The Crank-Nicolson scheme does not have a constraint on the time step size in order to achieve a stable solution. Therefore, the meshfree methods are insensitive to Courant constraints also.

5. Case studies: engineered landfills

Modern landfills and lagoons widely utilise composite liners (*e.g.*, a geomembrane over compacted clay) but unfortunately there is a paucity of published field investigations that have examined contaminant transport through the complete geosynthetic composite liner system (Rowe *et al.* 2004). The understanding of factors associated with design for contaminant transport mitigation, selection of materials and long-term performance of composite liners has improved considerably over the last two decades. The importance of some of these factors can be best illustrated with reference to actual case records. Three case studies of contaminant transport through landfill liners are used to demonstrate the applicability and performance of the proposed RPIM. The case studies considered are: (1) The Confederation Road landfill (2) Keele Valley landfill, and (3) Performance of compacted clay liner portion in a composite landfill liner.

5.1 Case study 1: the confederation road landfill

A case study of the Confederation Road landfill reported in Quigley and Rowe (1986) has been considered. The site consists of ~7.5 m of domestic solid waste, with a 0.5 m clay cover, overlies homogeneous, massive grey silty clay. The waste projects about 2 m above the surrounding ground surface and was placed in a borrow trench excavated about 5.5 m into the original clay. The calculated effective stresses incorporate the effect of a slight regional downward gradient (i = 0.25) which creates a downward average linearised groundwater velocity of ~0.0024 m/year.

The in-situ vertical effective stress (σ_v') indicated that the clay is overconsolidated by about 90 kPa with a slight increase near the clay/waste interface where the moisture content decreases slightly from 23 to 21%. The desiccated crust is highly fissured in the upper 4 m of the brown oxidised clay and much less fissured from 4 to 6.5 m in the lower grey portion of the crust. At the interface, which is probably within 1 m of the base of the desiccated crust, no fissures are observed in the 50 or more boreholes drilled at the site.

The wastes included in the original published report are: sodium chloride, heavy metals, dissolved organic carbon and isotopes. In regard to the hydraulic conductivity of a contaminated clay liner (CCL), an interdisciplinary study was published by Quigley *et al.* (1987) appears to be one of the very few scientific field studies performed. The study employed municipal solid waste (MSW)

Table 1 Data used for case study of the Confederation Road landfill

Parameter	Value	
	Chloride	Sodium
Seepage velocity (m/year)	0.0024	0.0024
Length of the reach (m)	3.0	3.0
Dispersion coefficient (m^2/year)	0.02	0.012
Retardation coefficient	1.0	1.46
Total duration of simulation (years)	15	15
Time step (Δt) (year)	0.5	0.5
Number of divisions in length direction	10	10
Pore water concentration (mol/m^3)	34	24

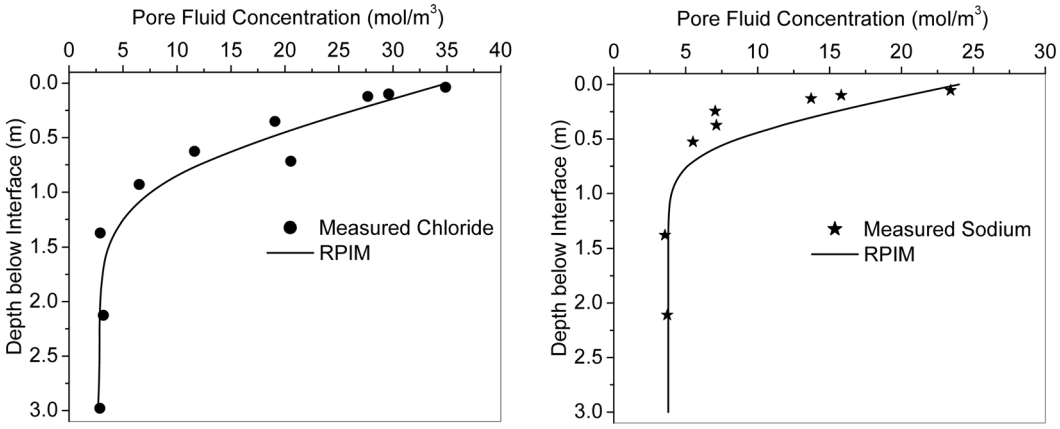

Fig. 6 Pore fluid concentrations of Cl^- and Na^+ in clay below waste after 15 years: RPIM and field data

leachate as the permeant and it confirms that the leachate did not increase the hydraulic conductivity of inactive barrier clay. The hydraulic conductivity profiles show approximately constant values except within about 20 cm of the clay/water interface where a slight decrease is observed. This case study example is used for modelling of contaminant transport through the clay liner using the RPIM.

In RPIM, the domain [0, 3 m] is divided into 11 uniformly spaced nodes with 10 cells. The parameters used in the analysis are given in Table 1. For modelling contaminant migration through the landfill liner, it was assumed that the influent concentration was constant at C_0 and the boundary is located at the infinitely thick layer of the porous medium. In Fig. 6, the spatial solute distribution curves obtained from the RPIM are compared with the pore fluid concentrations of chloride and sodium obtained from the field investigation. From the figure it is observed that the results are agreeing well with the field data.

5.2 Case study 2: Keele Valley landfill

A case study of the Keele Valley landfill reported in King *et al.* (1993) has been considered. The Keele Valley landfill at Maple, Ontario, approximately 10 km north of Metropolitan Toronto, is owned and operated by the Municipality of Metropolitan Toronto Department of Works. The landfill is used for the disposal of domestic, commercial and non-hazardous wastes. The site is a 99-ha facility with a design capacity of approximately 20 Mt of refuse. The landfill occupies sand and gravel pits that ranges up to 30 m in depth and is located on the southern slope of Oak Ridges Moraine.

Due to the existence of an exploited groundwater resource down gradient of the site, a compacted, natural clayey soil liner and leachate collection system are provided for the landfill with the purpose of reducing the potential environmental impact by leachate on the underlying aquifers. Nine conductivity sensor sets had been installed at 75 mm vertical interval at nine locations in the liner to monitor the expected slow advance of mobile chemicals from the leachate by diffusion and advection.

With low hydraulic conductivity values of 10^{-8} cm/s and low hydraulic heads, very low seepage velocities will exist in the Keele Valley liner. At the lysimeter locations, the thinner liners of 30-50

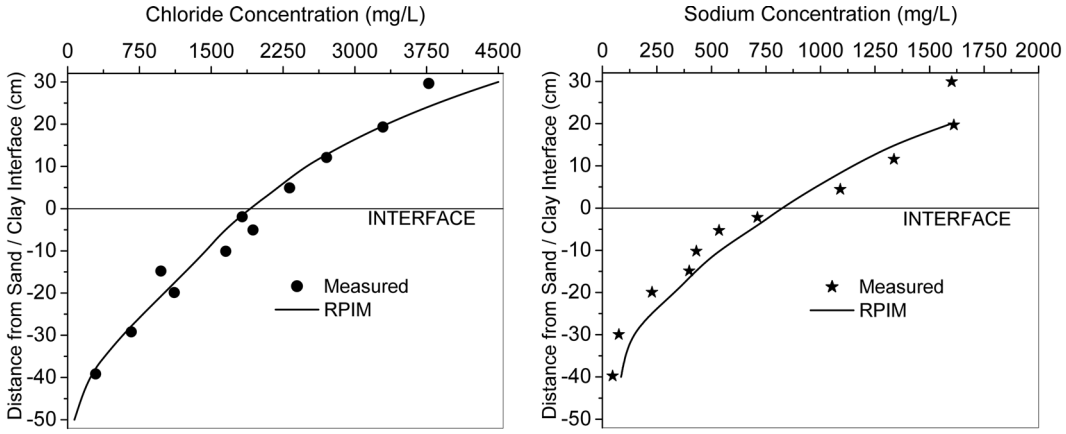

Fig. 7 Pore fluid concentration profiles for chloride and sodium ions at 4.25 years, Keele Valley landfill: RPIM and field data

cm result in higher gradients for the leachate heads of 40 and 200 cm, and advective seepage velocities of ~2.5-8 cm/year are calculated. To determine the extent of leachate migration, several areas of liner exposed to leachate were uncovered and examined. Pore water was obtained from slices of the brown clayey till liner samples by high-pressure squeezing and consolidation at 30 MPa. Measured concentration profiles are presented in Fig. 7, for a post construction diffusive time of 4.25 years. A chloride ion diffusion profile and a series of cation diffusion profiles have been obtained at the Metropolitan Toronto and Keele Valley landfill site. The reported results for chloride show a smooth curve starting at the top of the sand layer and extending a total distance of 70-75 cm over a period of 4.25 years. A diffusion profile fitted to the data assuming negligible advection yielded a field value for diffusion coefficient (D_{cl}) $\approx 6.5 \times 10^{-10}$ m^2/s. The presence of diffusion profiles in the sand layer can be attributed to the effects of biological clogging of the upper portion of the sand layer very shortly after waste placement began.

In the RPIM, the domain [0, 80 cm] is divided into 21 uniformly spaced nodes with 20 cells. The

Table 2 Data used for case study of the Keele Valley landfill

Parameter	Value	
	Chloride	Sodium
Hydraulic conductivity (m/year)	0.0015	0.0015
Length of the reach (cm)	80	80
Dispersion coefficient (cm^2/year)	205	47
Retardation coefficient	1.0	1.46
Total duration of simulation (years)	4.25	4.25
Time step (Δt) (year)	0.85	0.85
Number of divisions in length direction	20	20
Initial concentration (mg/l)	50	-
Concentration at source boundary (mg/l)	4500	1600

parameters used in the analysis are given in Table 2. The spatial solute distribution curves obtained from the RPIM are compared with the pore fluid concentrations of chloride and sodium obtained from the field investigation (Fig. 7). Based on the graphical comparison, it is observed that the results of the RPIM are agreeing well with the field investigation data.

5.3 Case study 3: performance of compacted clay liner portion in a composite landfill liner

The lagoon under study was situated in a landfill located in Ontario, Canada (Lake and Rowe 2005). Non-hazardous industrial, municipal and commercial wastes were being placed in this multi-cell landfill that is lined with a compacted clay liner and leachate collection system. Below the landfill lies the Rochester Shale formation, consisting of thin beds of aphanitic shales and shaley dolostones. The original location of the lagoon was temporary and served the landfill for 14 years at which time a new lagoon was constructed and the original lagoon decommissioned.

Lagoon storage capacity was approximately 2500 m^3 (side slopes of 3:1) and were lined with a 1.5 mm high density polyethylene (HDPE) geomembrane over a compacted clay liner (2.9 m thick) situated above the quarry's shale floor. Leachate height in the lagoon averaged 3 m above the bottom of the lagoon. The water table in the shale was estimated at approximately 3 m below the bottom of the compacted clay. Lysimeters have been installed under the clay liner of the lagoon and landfill to monitor leachate constituents migrating through the liners.

Investigation of the geomembrane revealed 82 cracks, holes and patches over a total area of 1350 m^2 (600 defects per hectare for the 14 year period of operation of the lagoon) after decommission. Even though the majority of the holes, cracks and patches were above the leachate levels in the lagoon, the defects below the leachate level appear to have been sufficient to allow leachate to migrate between the geomembrane and clay under low effective stress conditions.

Continuous, 75 mm diameter soil samples were taken of the compacted clay liner at the base of the lagoon at five locations with sampling depths ranging from 1.1-2.1 m. The soil was visually classified as light brown clay of low plasticity during sampling with no indication of fractures present. Pore water samples for each borehole (at various depths) were obtained using a pneumatic pore squeeze apparatus by applying 25 MPa pressure to the selected soil samples. Pore water

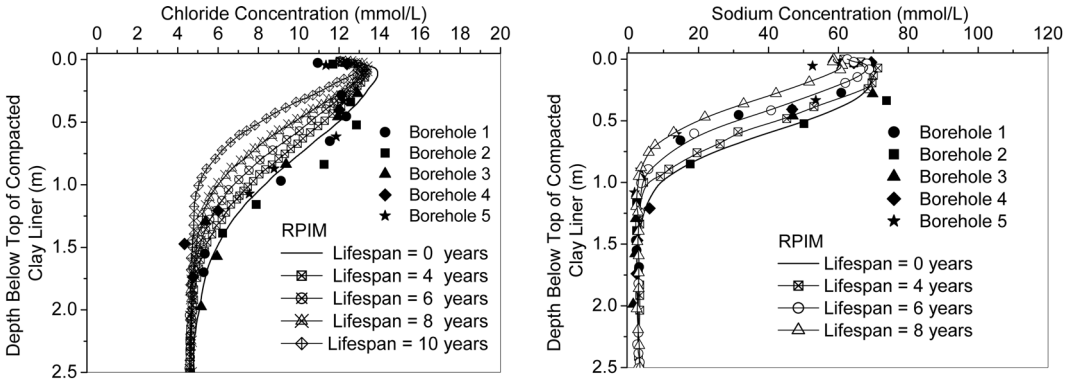

Fig. 8 Chloride and sodium concentration profiles through compacted clay liner for different lifespan of the geomembrane

Table 3 Data used for case study 2: CCL

Parameter	Value	
	Chloride	Sodium
Darcy velocity (m/year)	0.13	0.13
Porosity		
0.00-0.25 m	0.48	0.48
0.25-0.50 m	0.42	0.42
0.50-2.50 m	0.38	0.38
Dry density (g/cm^3)		
0.00-0.25 m	1.4	1.4
0.25-0.50 m	1.5	1.5
0.50-2.50 m	1.7	1.7
Leachate lagoon concentration (mol/m^3)		
0-4.5 years	7.17	61.95
4.5-9.0 years	17.37	150
9.0-14.0 years	14.57	46.86
Effective dispersion coefficient (m^2/year)	0.022	0.013
Distribution coefficient (cm^3/g)	0	0.2
Depth of compacted clay liner (m)	2.5	2.5
Total duration of simulation (years)	14	14
No. of divisions in length direction	20	20
Time step (Δt) (year)	0.5	0.5

obtained from the samples was analysed for sodium, potassium, magnesium and calcium using an atomic absorption spectrometer and chloride using a specific ion electrode.

Fig. 8 illustrate the pore fluid concentration profiles for chloride and sodium through the compacted clay liner at each borehole. When comparing boreholes data, there is some scatter, possibly the result of non-uniform distribution of defects found on the geomembrane liner (holes, tears, wrinkles) occurring at different time periods, producing differences in ionic pore water concentrations between boreholes. Also of note is the apparent back diffusion of chloride and sodium and possibly calcium, potassium and magnesium from the compacted clay into the lagoon.

For contaminant migration through the compacted clay liner, the top boundary condition was assumed to be of constant concentration for each of the three different time periods, *i.e.*, 0-4.5 years, 4.5-9.5 years and 9.5-14 years. The liner was considered to be infinitely thick and a constant concentration gradient was assumed at the bottom boundary for modelling purposes.

Geometric mean values of chloride and sodium concentrations in leachate lagoon for three time periods are presented in Table 3 along with the other parameters considered in the analysis for calculating the concentrations in the compacted clay liner. To evaluate the effectiveness of the geomembrane, contaminant transport modelling using the RPIM is performed for five different time periods, i.e., 0, 4, 6, 8 and 10 years, assuming that the geomembrane ceased to be effective and allowed leachate into direct contact with the clay liner. To account for back-diffusion of ions for the one month prior to the field investigation, it was assumed that dilution of the small amount of liquid at the bottom of the lagoon during this time caused a linear decrease in leachate concentrations of 20% over this time period.

In the meshfree model, the domain [0, 2.5] is discretised into 20 cells. A time step (Δt) of 0.5 year is used in the simulation. In Fig. 8, the spatial solute distribution curves obtained from the meshfree method are compared with the pore fluid concentrations obtained from the field investigation. A comparison of the observed chloride and sodium profiles with the meshfree results (Fig. 8), assuming that the geomembrane is ineffective at different times after construction suggests that the geomembrane ceased functioning effectively somewhere between 0 and 4 years after construction, which is in concordance with the findings of Lake and Rowe (Lake and Rowe 2005). It should be stated that the RPIM performed well for the case study data also. Thus, it ensures confidence in the use of these methods in contaminant transport modelling.

6. Conclusions

The RPIM with polynomial reproduction and its numerical implementation for modelling one-dimensional contaminant transport through the saturated porous media and landfill liners are presented. Shape functions based on 1D local support domain are constructed using the TPS-RBFs augmented with polynomials. A complete formulation of the RPIM is provided for the one-dimensional problems that can handle all types of boundary conditions. It is noted that the enforcement of essential boundary conditions in the RPIM is similar as in the conventional FEM. Numerical results obtained from the MATLAB program, developed for the RPIM are compared with the analytical and finite element results for different types of one-dimensional contaminant transport processes that occur in the saturated porous media. The results of the RPIM agree very well with those obtained from the analytical solutions, thus ensures the accurate formulation of the RPIM for contaminant transport modelling. The proposed RPIM generated results with no oscillations and thus the RPIM can be used in the case of highly advective flow systems. The practical applicability of the RPIM is demonstrated with three case studies of contaminant transport through landfill liners.

References

Belytschko, T., Lu, Y.Y. and Gu, L. (1994), "Element-free Galerkin methods", *Int. J. Numer. Meth. Eng.*, **37**(2), 229-256.

Boztosun, I. and Charafi, A. (2002), "An analysis of the linear advection-diffusion equation using mesh-free and mesh-dependent methods", *Eng. Anal. Bound. Elem.*, **26**(10), 889-895.

Craig, J.R. and Rabideau, A.J. (2006), "Finite difference modelling of contaminant transport using analytic element flow solutions", *Adv. Water Resour.*, **29**(7), 1075-1087.

Crank, J. (1956), *The mathematics of diffusion*, Oxford Press, London.

Dai, K.Y., Liu, G.R., Lim, K.M., Han, X. and Du, S.Y. (2004), "A meshfree radial point interpolation method for analysis of functionally graded material (FGM) plates", *Comput. Mech.*, **34**(3), 213-223.

Donea, J. and Huerta, A. (2003), *Finite element methods for flow problems*, John Wiley and Sons Inc., New York.

Eldho, T.I. and Rao, B.V. (1997), "Simulation of two-dimensional contaminant transport with dual reciprocity boundary elements", *Eng. Anal. Bound. Elem.*, **20**(3), 213-228.

Frind, E.O. (1988), "Solution of the advection–dispersion equation with free exit boundary", *Numer. Method Partial Differ. Equ.*, **4**(4), 301-313.

GeoSlope International Ltd. (2007), *Transport modelling with CTRAN/W 2007: an engineering methodology*,

Student version 7.02, 2nd Edition, Alberta, Canada.
King, K.S., Quigley, R.M., Fernandez, F., Reades, D.W. and Bacopoulos, A. (1993), "Hydraulic conductivity and diffusion monitoring of the Keele Valley Landfill liner, Maple, Ontario", *Can. Geotech. J.*, **30**(1), 124-134.
Lake, C.B. and Rowe, R.K. (2005), "The 14-year performance of a compacted clay liner used as part of a composite liner system for a leachate lagoon", *Geotech. Geol. Eng.*, **23**(6), 657-678.
Li, J., Chen, Y. and Pepper, D. (2003), "Radial basis function method for 1-d and 2-d groundwater contaminant transport modelling", *Comput. Mech.*, **32**(1-2), 10-15.
Liu, G.R., Zhang, G.Y., Gu, Y.T. and Wang, Y.Y. (2005), "A meshfree radial point interpolation method (RPIM) for three-dimensional solids", *Comput. Mech.*, **36**(6), 421-430.
Liu, W.K., Jun, S. and Zhang, Y.F. (1995), "Reproducing kernel particle methods", *Int. J. Numer. Meth. Fl.*, **20**(8-9), 1081-1106.
Monaghan, J.J. (1998), "An introduction to SPH", *Comput. Phys. Commun.*, **48**(1), 89-96.
Ogata, A. and Banks, R.B. (1961), *A solution of the differential equation of longitudinal dispersion in porous media,* USGS, Professional Paper: 411-A, Reston, VA.
Pinder, G.F. and Gray, W.G. (1977), *Finite element simulation in surface and subsurface hydrology*, Academic Press, New York.
Praveen Kumar, R. (2008), *Modelling of 1d, 2d and 3d contaminant transport through saturated and unsaturated porous media using meshfree techniques*, Ph.D. Thesis, Indian Institute of Technology Madras, India.
Praveen Kumar, R. and Dodagoudar, G.R. (2008), "Two-dimensional modelling of contaminant transport through saturated porous media using the radial point interpolation method (RPIM)", *Hydrogeol. J.*, **16**(8), 1497-1505.
Praveen Kumar, R., Dodagoudar, G.R. and Rao, B.N. (2007), "Meshfree modelling of one dimensional contaminant transport in unsaturated porous media", *Geomech. Geoeng.*, **2**(2), 129-136.
Quigley, R.M. and Rowe, R.K. (1986), *Leachate migration through clay below a domestic waste landfill, Sarnia, Ontario, Canada: chemical interpretation and modelling philosophies*, In: Lorenzen, D., Conway, R.A., Jackson, L.P., Hamza, A., Perket, C.L., Lacy, W.J. (eds) Hazardous and Industrial Solid Waste Testing and Disposal, Sixth Volume, ASTM STP 933, 93-103, American Society for Testing and Materials, Philadelphia, USA.
Quigley, R.M., Fernandez, F., Yanful, E., Helgason, T., Margaritis, A. and Whitby, J.L. (1987), "Hydraulic conductivity of contaminated natural clay directly beneath a domestic landfill", *Can. Geotech. J.*, **24**(3), 377-383.
Rowe, R.K. and Booker, J.R. (1985), "1-d pollutant migration in soils of finite depth", *J. Geotech. Eng. - ASCE*, **111**(4), 479-499.
Rowe, R.K., Quigley, R.M., Brachman, R.W.I. and Booker, J.R. (2004), *Barrier systems for waste disposal*, E & FN Spon Press, London.
van Genuchten, M.Th. (1981), "Analytical solutions for chemical transport with simultaneous adsorption, zero-order production and first-order decay", *J. Hydrol.*, **49**(3-4), 213-233.
Wang, J.G. and Liu, G.R. (2002), "On the optimal shape parameters of radial basis functions used for 2-d meshless methods", *Comput. Method. Appl. M.*, **191**(23-24), 2611-2630.
Wang, J.G., Liu, G.R. and Lin, P. (2002), "Numerical analysis of Biot's consolidation process by radial point interpolation method", *Int. J. Solids Struct.*, **39**(6), 1557-1573.
Zheng, C. and Bennett, G.D. (1995), *Applied contaminant transport modelling: theory and practice*, Van Nostrand Reinhold, New York.

PL